Navier-Stokes High-Lift Airfoil Computations with Automatic Transition Prediction using the DLR TAU Code

A. KRUMBEIN[1] and N. KRIMMELBEIN[2]
[1]Deutsches Zentrum für Luft- und Raumfahrt e.V., AS-NV, Bunsenstraße 10,
D-37073 Göttingen, Germany, andreas.krumbein@dlr.de
[2]Technical University of Braunschweig, ISM, Bienroder Weg 3,
D- 38106 Braunschweig, Germany, n.krimmelbein@tu-braunschweig.de

Summary

A Reynolds-averaged Navier-Stokes solver, a laminar boundary-layer code and different transition prediction methods for the prediction of Tollmien-Schlichting and cross flow instabilities were coupled for the automatic prediction of laminar-turbulent transition on general 3-dimensional aircraft configurations during the ongoing computation of the flow. The prediction procedure is applied to a two-dimensional three-element high-lift airfoil configuration which is characterized by the existence of laminar separation bubbles using different operation modes of the procedure.

1 Introduction

The modelling of laminar-turbulent transition in Reynolds-averaged Navier-Stokes (RANS) solvers is a crucial issue when high quality simulation results for aircraft shall be produced. Especially the simulation of flows around high-lift systems of aircraft may result in significant errors when the transition points are of insufficient accuracy or are not taken into account at all. High-lift systems very often involve multi-component wings (e.g. slat, main wing, and flaps) and may have very high levels of total circulation. Because all components of the high-lift system are in close interaction with one another the total circulation and the complete flow field is affected by one transition line on one of the components.

Although the overall lift value may be predicted with satisfactory accuracy slight deviations between the real and the computed pressures can lead to large errors in the computed overall drag value. It could be shown that the overall pressure drag of a high-lift configuration, which dominates the drag value of the configuration as a whole as well as the drag of every single element, is composed of a balance of very large positive and negative contributions. The contribution of one single element may be one order of magnitude larger than the resulting overall drag of the complete configuration. Thus, a relative error of 5% of the computed drag on the slat upper side may result in a change of 50% for the overall drag value.

Another aspect of taking into account transition is that in many cases the high potential of higher order turbulence models can be made use of only when the areas of laminar-turbulent transition are known and deployed in the computational procedures with sufficiently high accuracy. Thus, in modern computational fluid dynamics (CFD) tools a robust transition modelling must be established together with reliable and effective turbulence models. Only if the transition locations are taken into account with sufficient accuracy all physical characteristics of the flow field can be reproduced in such a way that the demanding quality requirements of

the industry are satisfied.

For the design process of wings in industry, there exists the demand for a RANS-based CFD tool that is able to handle flows automatically and autonomously with laminar-turbulent transition. Existing transition prediction methods vary from empirical transition criteria via the local, linear stability equations based on small disturbance theory or non-local, linear and non-local, non-linear stability methods using the parabolized stability equations over large eddy simulations to direct numerical simulations of the Navier-Stokes equations. Empirical transition criteria and the e^N-method [1],[2] based on local, linear stability theory and the parallel flow assumption represent *state-of-the-art* methods for the prediction of transition onset in many industrial applications. Although they do not account for a number of fundamental aspects in the transition process e^N-methods are used in aircraft industry most frequently for design purposes covering transition due to Tollmien-Schlichting (TS) and cross flow (CF) instabilities. Because there are no other practical methods presently available for industrial applications e^N-methods together with the two-*N*-factor method and empirical criteria for transition mechanisms which are not covered by the e^N approach (e.g. bypass and attachment line transition) are going to be used further on for the design of aircraft wings and wing systems even for a future laminar wing of transport type aircraft.

Recently the unstructured/hybrid RANS solver TAU [3] of the Deutsches Zentrum für Luft- und Raumfahrt, German Aerospace Center (DLR) has been provided with a general transition prediction functionality which can be applied to general 3-dimensional aircraft configurations. The developments and first technical validation steps have carried out at the Institute of Fluid Mechanics of the Technical University of Braunschweig, [4],[5]. The TAU code is used together with the laminar boundary-layer method in [6] and the local linear stability code in [7]. These two codes and an infrastructure part of the TAU code are components of a so called ‘transition prediction module’ that is coupled to the RANS solver and that interacts with the RANS solver during the computation in a very similar way as it is documented in [8].

For a long time it was necessary to use transition database methods in order to apply the e^N-method for transition prediction in a fully automatic way so that the transition location iteration could be executed without intervention (automatic) by the user of the RANS code and without *a priori* knowledge of the transition characteristics of the specific flow problem (autonomous). Now the fully automated local, linear stability solver in [7] is available using a frequency estimator for the detection of the relevant regions of amplified disturbances for TS instabilities and a wave length estimator for CF instabilities.

In this paper the coupling structure between the TAU code and the transition prediction module is outlined and the transition prediction strategy is described together with the different operation modes of the transition prediction module which can be selected by the user. The main objective is to demonstrate the different characteristics of the different operation modes and their impact on the computational results which are obtained for a two-dimensional three-element high-lift airfoil configuration which is characterized by the existence of laminar

separation bubbles for the flow case presented. The computational results are compared to experimental findings.

2 Transition Prediction Coupling

On the one hand, the transition prediction module consists of an infrastructure part inside the flow solver which performs preprocessing operations necessary for each step of the transition prediction procedure, for example the extraction of the surface pressure distribution from a wing section. On the other hand, the module contains a number of additional components which basically execute the transition prediction. These additional components are a laminar boundary-layer code for swept, tapered wings [6], two e^N-database methods, one for TS and the other for CF instabilities [9],[10] and a local, linear stability code [7].

With respect to the calculation of the laminar boundary-layer (*BL*) parameters the coupled system can be run in two different modes: Either the TAU code communicates the surface pressure distribution of the configuration to the laminar boundary-layer method, the laminar boundary-layer method then computes all of the boundary-layer parameters that are needed for a selected transition prediction method and the transition prediction method determines new transition locations that are given back to the RANS solver (*BL mode 1*). Or the TAU code computes the necessary boundary-layer parameters internally and communicates them directly to the transition prediction method (*BL mode 2*).

Also with respect to the transition prediction (*PD*) method, the system can be run in two different modes: Either the two e^N-database methods (*PD mode 1*) or the local, linear stability code (*PD mode 2*) can be used for the determination of transition points due to TS or CF waves.

This coupled structure results in an iteration procedure for the transition locations within the iterations of the RANS equations. The structure of the approaches using the two different *BL modes* is outlined graphically in Fig. 1.

During the computation, the RANS solver is stopped after a certain number of iteration cycles usually when the lift has sufficiently converged, that is when pressure oscillations have been damped to a sufficiently low degree. Then the transition module is called, geometrical data are processed and all laminar viscous data – basically the velocity profiles in streamwise and crossflow direction and their 1st and 2nd derivatives – are calculated either by the boundary-layer code or by the TAU code itself. Then, either the two e^N-database methods or the stability code analyze the laminar boundary layer and try to determine a transition point. For *BL mode 1* this is possible only when the transition point is located upstream of the separation point predicted by the boundary-layer code because the boundary-layer code terminates when a separation is detected. If a transition point due to TS or CF instabilities was found it is communicated back to the RANS solver. If no transition point due to TS or CF instabilities upstream of the laminar separation point could be found the laminar separation point is used as approximation of the real transition point. This is an attempt to predict transition due strictly to the presence of separation bubbles. This approach often yields a good approximation of the real transition point when transition does not occur before the laminar boundary layer separates, particularly for low Reynolds number

flows. For *BL mode 2* the laminar boundary-layer data are calculated beyond the point of laminar separation which is detected by the TAU code inside the RANS computational grid. Thus, transition inside laminar separation bubbles can be detected without relying on an approximation. Practically, the determination of transition inside laminar separation bubbles is only realizable using *PD mode 2* because the e^N-database methods do not contain enough information for all possible characters which a laminar separation bubble can exhibit.

These steps are done for the upper and lower sides of all specified wing sections. When all new transition locations have been communicated back to the RANS solver, each transition location is slightly underrelaxed to damp oscillations in the convergence history of the transition locations. Then, all underrelaxed transition points – they represent a transition line on the upper or lower surface of a wing element in form of a polygonial line – are mapped into the surface grid of the configuration applying a transition setting algorithm subdividing the surface of the geometry into laminar and turbulent regions, and the computation is continued. In so doing, the determination of the transition locations becomes an iteration process itself. With each transition location iteration step the underrelaxation factor is reduced until a converged state of all transition points has been obtained.

3 Computational Results

The system was applied to the A310 take-off configuration [11] consisting of slat, main airfoil and flap defined by M = 0.221, Re = 6.11 x 10^6 and α = 21.40°. According to [12], as value for the limiting N-factor of the TS-database method N_T = 9 was used. In the experiments [11] the following transition locations were determined on the upper sides of the slat, $(x^T_{upp}/c)_{slat}$ = 0.15, and the flap, $(x^T_{upp}/c)_{flap}$ = 0.345. On the main airfoil upper side the transition location was not measured, but the location of the upper side kink – the point where the slat trailing edge is located when the configuration is undeflected – is useful as a point of orientation, $(x^{kink}_{upp}/c)_{main}$ = 0.19. On the lower sides, the transition points were not measured. In the computations a standard one-equation turbulence model was applied. The computations were started from scratch and were carried out for two different computational grids [13] exhibiting different grid densities. In the fine grid, the grid resolution was highly increased compared to the coarse grid in streamwise as well as in wall normal direction in the structured parts which resolve the boundary layers. While the coarse grid (grid 1) consists of about 22,000 primary grid points that fine grid (grid 2) has about 122,000 points, Fig. 2. Because in the experiments a laminar separation bubble on the slat upper side caused transition, the computations using grid 2 were intended to resolve the laminar separation bubble and to investigate the impact on the transition locations caused by the different modes of transition prediction module.

The three different combinations of modes which are currently available in the TAU code for 2-dimensional cases were applied: a) *BL mode 1* & *PD mode 1*, b) *BL mode 1* & *PD mode 2* and c) *BL mode 2* & *PD mode 2*.

For grid 1, the transition prediction procedure which was started with initial transition points located almost at the upper side trailing edges of the particular elements (on the lower sides, fully laminar flow was assumed up to the trailing

edges) was run with a pre-prediction phase of 1000 iteration cycles where the laminar separation points which occur in the RANS grid are used as transition points in order to stabilize the computation. The pre-prediction interval was 20 iteration cycles. Then, the transition prediction iteration was started using a prediction interval of 500 iteration cycles. While for the mode combinations a) & b) the results are identical, for mode combination c) it was found that the transition location iteration could not converge because the computational grid was not fine enough. This outcome is due to the following: After a certain number of iteration steps a transition point on the main element upper side is found located only 5 grid points downstream of the pressure minimum. At a later stage of the computation, due to the upstream influence in the numerical procedure of the RANS solver no fully laminar BL velocity profiles with adverse pressure gradient exist in that area anymore, so that the linear stability code can not detect amplified disturbances which could lead to transition.

In Fig. 3, the c_p- and c_f-distributions for grid 1 are shown. As expected, the results from the computations with predicted transition (PD) yield more negative pressure levels on the upper sides of all elements than the fully turbulent (FT) results. This effect is pronounced in the suction peak areas. The comparison of the c_f-distributions clearly shows the transition from laminar to turbulent flow on all elements. On the main wing element transition occurs directly upstream of the kink, on slat and flap upper side the predicted transition points are located upstream of the experimentally determined locations.

Fig. 4 shows the results for grid 2. For grid 2 all three mode combinations yield converged results and again the results of the mode combinations a) & b) are identical. For the computations with transition, a separation bubble on the slat upper side is reproduced. For a) & b), where the transition point inside the separation bubble was approximated using the laminar separation point from the boundary-layer code, the resulting bubble is of too small extent and strength due to the fact that through the approximation the turbulence production starts too far upstream, so that the separation bubble can not fully develop. For mode combination c), where the stability analysis is carried out inside the laminar separation bubble, the extent and strength of the bubble show a good qualitative agreement with the experimental pressures. Whereas for a) & b) the predicted transition location on the slat upper side is not very different from that in grid 1, for mode combination c) the measured transition point now is reproduced with excellent accuracy. The transition point on the main wing element is determined downstream of the kink using a) & b) and more upstream of the kink than it was the case for grid 1 when combination c) is used. In the transition region on the main element, the interaction between transition and the influence of the kink lead to a relatively strong change between the c_f-distributions from mode combinations a) & b) on the one hand and from c) on the other hand. On the flap upper side the transition point resulting from a) & b) shows almost the same deviation from the measured value as for grid 1. For mode combination c) however a visible downstream shift of the transition point occurs decreasing the gap between the former computational results and the experiment without showing a separation. In Figs. 5 and 6, the velocity profiles in the region of the separation bubble on the

slat and in the area of the transition point on the flap are shown. The corresponding transition locations are marked. A close inspection of the grid and the velocity profiles in the transition region on the flap upper side reveals that the boundary layer is shortly before separation. Possibly, a separation existed on the flap during the experiment which can not be resolved by the cell density in this area of grid 2. Very probably, a finer streamwise grid resolution in this area will lead to a better result and yield an improved prediction of the transition location on the flap.

4 Conclusion

The TAU code coupled to a newly developed transition prediction module was applied to a two-dimensional three-element high-lift airfoil configuration which is characterized by the existence of laminar separation bubbles. The prediction of the transition location was carried out in a fully automatic manner during the ongoing RANS computation so that no intervention of the user is needed. It could be shown that when the computational grid is fine enough transition locations inside laminar separation bubbles can be predicted with high accuracy while the separation bubble itself can reproduced well with respect to its extent and strength.

Acknowledgements

This work has been carried out within the NRC-HGF project 'RANS Simulation of Reynolds Number Effects on Airfoil Stall'. This project is a collaboration between the Institute for Aerospace Research (IAR) of the National Research Council Canada (NRC), the Institute of Fluid Mechanics of the Technical University of Braunschweig (TU-BS) and the Institute of Aerodynamics and Flow Technology of the German Aerospace Center (DLR). The project was managed by TU-BS and funded by the Helmholtz-Gemeinschaft Deutscher Forschungszentren (HGF). The development work within the TAU code was carried out by TU-BS within the German Research initiative MEGADESIGN.

References

[1] Smith, A.M.O., Gamberoni, N., "Transition, Pressure Gradient and Stability Theory", Douglas Aircraft Company, Long Beach, Calif. Rep. ES 26388, 1956.

[2] van Ingen, J.L., "A suggested Semi-Empirical Method for the Calculation of the Boundary Layer Transition Region", University of Delft, Dept. of Aerospace Engineering, Delft, The Netherlands, Rep. VTH-74, 1956.

[3] Kroll, N., Rossow, C.-C., Schwamborn, D., Becker, K., and Heller, G., "MEGAFLOW - A Numerical Flow Simulation Tool For Transport Aircraft Design", ICAS Congress 2002 [CD-Rom], ICAS, Toronto, Canada, 2002, pp. 1.105.1-1.105.20.

[4] Nebel, C., Radespiel, R., and Wolf, T., "Transition Prediction for 3D Flows Using a Reynolds-Averaged Navier-Stokes Code and N-Factor Methods", AIAA-2003-3593.

[5] Krimmelbein, N., Radespiel, R., Nebel, C., "Numerical Aspects of Transition Prediction for Three-Dimensional Configurations", AIAA-2005-4764.

[6] "COCO – A Program to compute Velocity and Temperature Profiles for Local and Nonlocal Stability Analysis of Compressible, Conical Boundary Layers with Suction", ZARM Technik Report, November 1998.

[7] Schrauf, G., "LILO 2.1 User's Guide and Tutorial", Bremen, Germany, GSSC Technical Report 6, originally issued Sep. 2004, modified for Version 2.1 July 2006.

[8] Krumbein, A., "Automatic Transition Prediction and Application to 3D Wing Configurations", in print at *Journal of Aircraft*, DOI: 10.2514/2254; also AIAA Paper

2006-914, June 2006.

[9] Stock, H. W., Degenhardt, E., "A simplified e^N method for transition prediction in two-dimensional, incompressible boundary layers", *Zeitung für Flugwissenschaft und Weltraumforschung*, Vol. 13, 1989, pp. 16-30.

[10] Casalis, G., Arnal, D., "ELFIN II Subtask 2.3: Database method – Development and validation of the simplified method for pure crossflow instability at low speed", ELFIN II - European Laminar Flow Investigation, Technical Report n° 145, ONERA-CERT, Département d'Études et de Recherches en Aérothermodynamique (DERAT), R.T. DERAT nº 119/5618.16, December 1996.

[11] Manie, F., Piccin, O., Ray, J.P., "Test Report of the 2D Model M1 in the ONERA F1 Wind Tunnel", GARTEUR AD(AG-08), TP-041, 1989.

[12] Arthur, M. T., Dol, H., Krumbein, A., Houdeville, R., Ponsin, J., "Application of Transition Criteria in Navier-Stokes Computations", GARTEUR AD(AG-35), TP-137, 2003.

[13] Wild, J., private communications, DLR, Institute of Aerodynamics and Flow Technology, Braunschweig, Germany, Nov. 2003 & Nov. 2005.

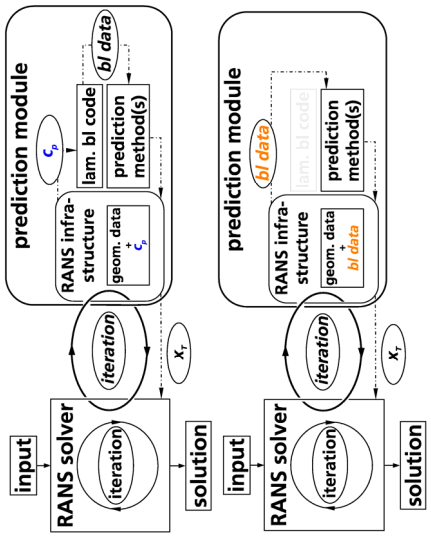

Fig. 1 Coupling structure: *BL mode 1* (left) and *BL mode 2* (right)

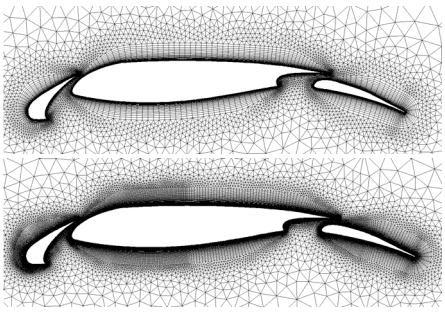

Fig. 2 Computational grids: grid 1 (above), grid 2 (below)

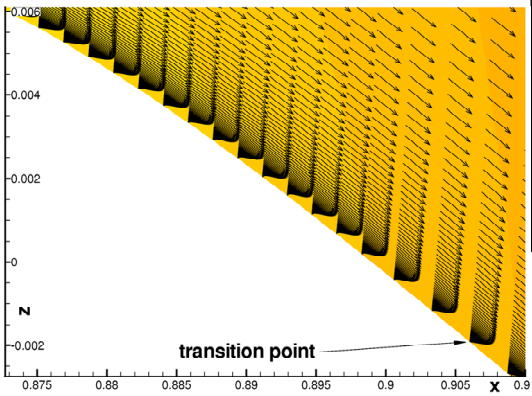

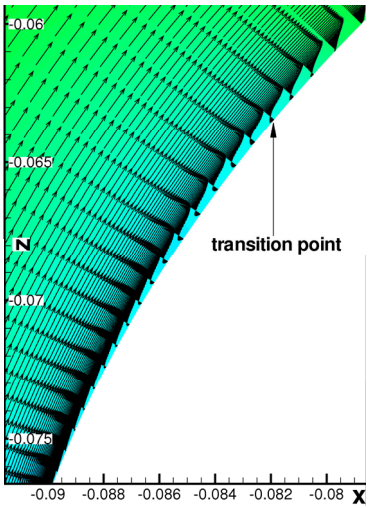

Fig. 5 Velocity profiles in the slat transition region

Fig. 6 Velocity profiles in the flap transition region, scales independent

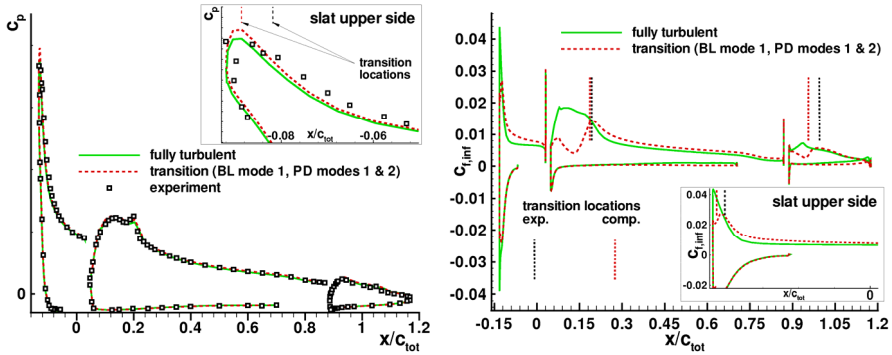

Fig. 3 c_p- (left) and c_f-distributions (right) for grid 1.

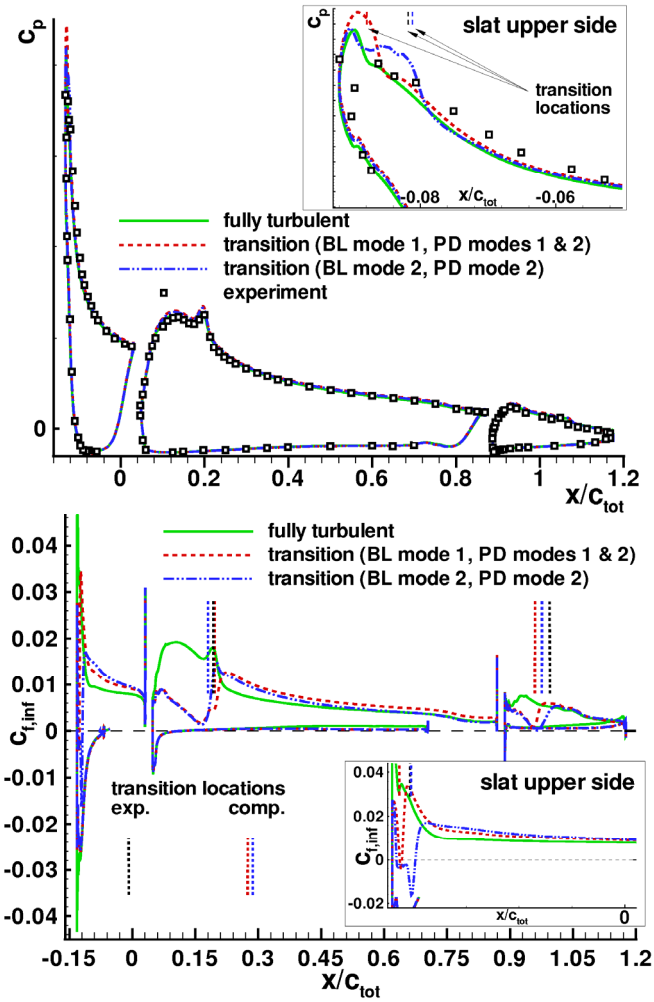

Fig. 4 c_p- (above) and c_f-distributions (below) for grid 2.